Heat Flow and Hydrothermal Circulation in the Cascade Range, North-Central Oregon

Author(s): S. E. Ingebritsen, D. R. Sherrod and R. H. Mariner

Source: *Science*, Mar. 17, 1989, New Series, Vol. 243, No. 4897 (Mar. 17, 1989), pp. 1458-1462

Published by: American Association for the Advancement of Science

Stable URL: https://www.jstor.org/stable/1703129

our one-dimensional model as long as the chain is allowed to fluctuate inside its tube.

The model presented here has two major advantages: (i) it is simple enough to be amenable to analytical analysis, and (ii) the effect of the internal modes can be singled out and interpreted by comparing the results of this model with those of the original biased reptation model (*10*), which replaces the springs by rigid rods. However, only longitudinal fluctuations (those along the tube axis) are allowed in this model, which clearly reduces the total effect of the fluctuations available to the molecule in a gel. Transverse fluctuations, including hernias, are expected to play an important role in this system, especially in high fields and for long molecules. Nonhomogeneous gels may also increase the effect of the fluctuations. Hernias may be responsible for U- and W-shaped conformations that can affect the mobility of DNAs in FIGE. Taking into account these two types of conformations would enhance the effect of the fluctuations and possibly increase the importance of the effects found upon field reversal; for example, the minima found on Fig. 2 would probably be deeper if more degrees of freedom would be allowed to the reptating fluctuating chains. The recent results of fluorescence-detected linear dichroism experiments can be interpreted in terms of intratube fluctuations (including both tube length fluctuations and nonhomogeneous spring stretching), and these fluctuations can explain the FIGE effect when the frequency of the pulsed field is in resonance with the relaxation time associated with the intratube fluctuations.

REFERENCES

1. D. C. Schwartz and C. R. Cantor, *Cell* **37**, 67 (1984).
2. G. F. Carle, M. Frank, M. V. Olson, *Science* **232**, 65 (1986).
3. P. Serwer, *Electrophoresis* **4**, 375 (1983); N. C. Stellwagen, *Biopolymers* **24**, 2243 (1985); M. Jonsson, B. Akerman, B. Norden, *ibid.* **27**, 381 (1988).
4. M. Lalande, J. Noolandi, C. Turmel, J. Rousseau, G. W. Slater, *Proc. Natl. Acad. Sci. U.S.A.* **84**, 8011(1987).
5. E. M. Southern, R. Anand, W. R. A. Brown, D. S. Fletcher, *Nucleic Acids Res.* **15**, 5925 (1987); P. Serwer, *Electrophoresis* **8**, 301 (1987); B. W. Birren, E. Lai, S. M. Clark, L. Hood, M. I. Simon, *Nucleic Acids Res.* **16**, 7563 (1988).
6. G. Holzwarth, C. B. McKee, S. Steiger, G. Crater, *Nucleic Acids Res.* **15**, 10031 (1987).
7. L. S. Lerman and H. L. Frisch, *Biopolymers* **21**, 995 (1982).
8. O. J. Lumpkin, P. Déjardin, B. H. Zimm, *ibid.* **24**, 1575 (1985).
9. G. W. Slater and J. Noolandi, *ibid.* **25**, 431 (1986); K. Kremer, *Polym. Commun.* **29**, 292 (1988).
10. J. Noolandi, J. Rousseau, G. W. Slater, C. Turmel, M. Lalande, *Phys. Rev. Lett.* **58**, 2428 (1987).
11. J. M. Deutsch, *Science* **240**, 922 (1988).
12. J.-L. Viovy, *Phys. Rev. Lett* **60**, 855 (1988).
13. M. Doi and S. F. Edwards, *The Theory of Polymer Dynamics* (Oxford Univ. Press, Oxford, 1986).
14. R. I. Tanner, *Engineering Rheology* (Oxford Univ. Press, Oxford, 1985).
15. G. Holzwarth, K. J. Platt, R. W. Whitcomb, C. B. Mckee, *Biophys. J.* **53**, 407a (1988).
16. C. J. Bostock, *Nucleic Acids Res.* **16**, 4239 (1988).

17 November 1988; accepted 2 February 1989

Heat Flow and Hydrothermal Circulation in the Cascade Range, North-Central Oregon

S. E. INGEBRITSEN, D. R. SHERROD, R. H. MARINER

In north-central Oregon a large area of near-zero near-surface conductive heat flow occurs in young volcanic rocks of the Cascade Range. Recent advective heat flux measurements and a heat-budget analysis suggest that ground-water circulation sweeps sufficient heat out of areas where rocks younger than 6 Ma (million years ago) are exposed to account for the anomalously high advective and conductive heat discharge measured in older rocks at lower elevations. Earlier workers have proposed that an extensive midcrustal magmatic heat source is responsible for this anomalously high heat flow. Instead, high heat flow in the older rocks may be a relatively shallow phenomenon caused by regional ground-water flow. Any deeper anomaly may be relatively narrow, spatially variable, and essentially confined to the Quaternary (less than 2 Ma) arc. Magmatic intrusion at a rate of 9 to 33 cubic kilometers per kilometer of arc length per million years can account for the total heat flow anomaly. Deep drilling in the areas of high heat flow in the older rocks could indicate which model is more appropriate for the near-surface heat flow data.

QUATERNARY VOLCANOES OF THE Cascade Range form a 1200-km-long volcanic arc that extends from southern British Columbia to northern California. The arc is related to subduction of the Juan de Fuca Plate beneath North America. Detailed geologic mapping, measurements of advective heat discharge, and numerous conductive heat flow measurements are available for a 135-km-long section of the Cascade Range in north-central Oregon. This data set allows us to estimate fluxes of heat and mass (thermal fluid and magma) and to document the role of ground-water movement in redistributing heat in the upper crust. The results provide some insight into the thermal structure of the arc, and have implications for its geothermal resource potential.

In the study area (Fig. 1), the High Cascades physiographic subprovince is a broad constructional ridge of upper Pliocene and Quaternary (<3.3 Ma) volcanic rocks surmounted by several Quaternary stratovolcanoes. The High Cascades are flanked by Oligocene to lower Pliocene volcanic rocks of the Western Cascades to the west and Deschutes basin to the east. Western Cascades rocks also underlie the High Cascades; they are generally less permeable than the younger rocks. In this report, we use Western Cascades and High Cascades as location terms. We also distinguish (i) the Quaternary (<2 Ma) arc, or area of Quaternary vents (Fig. 1), because older magmatic heat sources will generally have cooled to near ambient temperatures (*1*), and (ii) the region where uppermost Miocene (<6 Ma),

U.S. Geological Survey, Menlo Park, CA 94025.

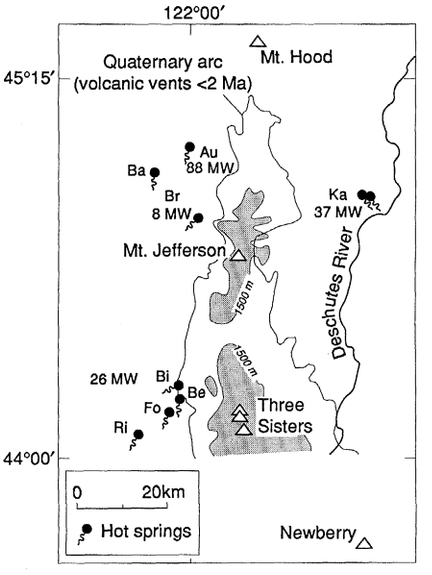

Fig. 1. Map showing the location of hot springs, the Quaternary arc, prominent volcanoes (△), the 1500-m-elevation contour, and the amount of heat transported advectively by the hot spring systems. The total for the southerly group of hot springs (~26 MW) is 1.5 times the value obtained from the individual spring groups (Table 1), because of diffuse input of thermal water into the surface drainage; hot springs: Au, Austin; Ba, Bagby; Br, Breitenbush; Bi, Bigelow; Be, Belknap; Fo, Foley; Ri, unnamed spring on Rider Creek; Ka, Kahneeta.

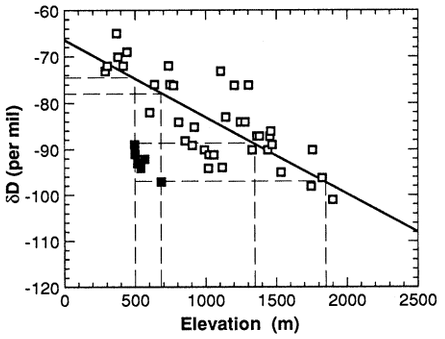

Fig. 2. Relation between deuterium content and elevation for waters on or west of the Cascade crest. Deuterium content (δD) is expressed as D/H ratios in per mil relative to SMOW (standard mean ocean water). Filled squares are from Na-Cl and Na-Ca-Cl thermal waters in the Western Cascades. Open squares are nonthermal samples from low-salinity springs and wells in zero- or first-order (unchanneled or headwater) basins on or west of the Cascade crest, and represent local meteoric water. Line is linear least square fit to these data. Because there is little oxygen shift in the thermal waters, $\delta^{18}O$ values show a similar pattern.

Pliocene, and Quaternary rocks are exposed, because their areal extent is roughly coincident with an extensive area of near-zero near-surface conductive heat flow (*2*).

Most of the thermal springs in the study area discharge in deep valleys in the Western Cascades up to 15 km west of the Quaternary arc. One set of thermal springs discharges from Oligocene or Miocene rocks 18 km east of the Quaternary arc (Fig. 1). No thermal springs occur in the Quaternary rocks. With two exceptions, the thermal waters are Na-Cl or Na-Ca-Cl waters. The ratios of Br to Cl are similar to those in seawater; these ratios and the high concentrations of Na and Cl (Table 1) suggest that the thermal waters may have circulated through rocks deposited in a marine environment. Thermal Na-Ca-Cl waters are typical of rift zones around the world, but in North America occur primarily in the Salton trough and in the Columbia embayment (*3*) of the Pacific Northwest.

The high Cl content of the thermal waters makes Cl a useful natural tracer, because surface waters in the Cascade Range of Oregon contain only about 0.5 mg liter^{-1} of Cl. The discharge of groups of thermal springs can be calculated by measuring the increased Cl load of streams passing through hot spring areas (*4*). In repetitions done on different occasions, these measurements (Table 1) have a reproducibility of ±10 to 15% or better, depending on the flow rate of the stream relative to the flow rate of the hot springs and on the Cl concentration in the thermal water.

The product of the measured hot spring discharge (Q), an appropriate density (ρ) and heat capacity (c), and the difference between a chemical geothermometer temperature (Table 1) and a reference temperature [$Q\rho c(T_g - 5°C)$] gives a measure of the heat transported advectively by the hot spring systems (Fig. 1). The total measured advective heat transport by thermal water in the study area is 159 MW (159×10^6 W). For comparison, the Quaternary magma extrusion rate of 3 to 6 km^3 per kilometer of arc length per million years (*5*) represents an average heat release of 60 to 120 MW in the study area (*6*).

The isotopic composition of the thermal waters in the Western Cascades indicates that they were recharged at relatively high elevations in the Quaternary arc, if the isotopic composition of precipitation has not changed significantly since the thermal waters were recharged. This would be the case if the thermal waters were recharged during the Holocene, as seems likely. The thermal waters are much more depleted isotopically than local meteoric waters in the Western Cascades. Their isotopic composition best matches that of meteoric waters at elevations of 1300 to 1900 m near the Cascade crest (Fig. 2). The hot springs are at elevations of 500 to 700 m. Thus an elevation difference of about 600 to 1400 m drives the thermal circulation systems.

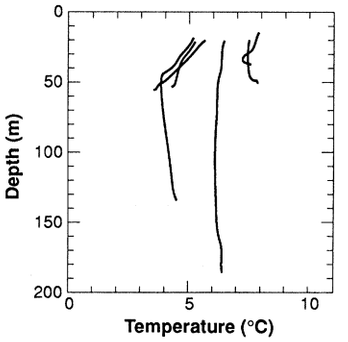

Fig. 3. Typical temperature-depth profiles from the Quaternary arc (*7, 8*), showing little or no temperature increase to depths of 150 m or more.

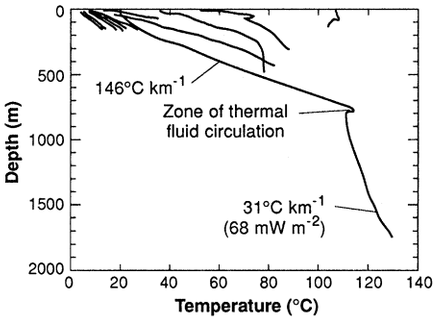

Fig. 4. Temperature-depth profiles from drill holes collared in rocks older than 6 Ma in the Breitenbush Hot Springs area (*8, 10, 11*). The deepest hole was completed to 2457 m, but was only logged to 1715 m. The bottom-hole (2457 m) temperature was >141°C (*26*). The gradient measured over the 1465- to 1715-m interval (31°C km^{-1}) projects to a bottom-hole temperature of 152°C.

The available data suggest that thermal waters recharged near the Cascade crest circulate to depth and flow laterally for distances of 10 to 20 km (Fig. 1) before discharging at relatively low elevations in the Western Cascades. Gravitationally driven thermal fluid circulation transports significant amounts of heat from the Quaternary arc into rocks older than 6 Ma and must profoundly affect the pattern of near-surface conductive heat flow. Gravitationally driven flow of lower temperature ground water must also transfer heat from the younger rocks to older rocks at lower elevations, but this effect is difficult to measure directly.

Conductive heat flow data (*7–11*) show that the Quaternary arc and adjacent 2- to 6-million-year-old volcanic rocks constitute a large area of near-zero near-surface conductive heat flow that results from downward and lateral flow of cold ground water (Fig. 3). In contrast, near-surface conductive heat flow is anomalously high in rocks older than 6 Ma exposed at lower elevations in the

Table 1. Geochemical and discharge data for hot springs in the study area. Dashes indicate lack of data. Hot spring locations are shown in Fig. 1.

Name	Q* (liter s^{-1})	T_d† (°C)	T_g‡ (°C)	Ca	Na	Cl	Br
				(mg liter^{-1})			
Austin	120	86	186	35	305	390	1.4
Bagby	1	58	52	3.3	53	14	–
Breitenbush	12	84	174	95	745	1200	5.0
Bigelow	–	59	155	195	675	1250	8.7
Belknap	18§	73	152	210	660	1200	5.4
Foley	9	79	100	510	555	1350	–
Unnamed on Rider Creek	5	46	135	215	405	790	2.4
Kahneeta	69	83	137	13	400	240	–

*Discharge based on chloride-flux measurements, except for Bagby Hot Spring, where discharge was measured directly. †Discharge temperature. ‡Chemical geothermometer temperatures based on anhydrite saturation (*24*), except for Kahneeta and Bagby, which are based on the silica and cation geothermometers (*25*). §Combined discharge of Bigelow and Belknap Hot Springs.

Western Cascades (Fig. 4). A similar pattern of low-to-zero conductive heat flow in permeable volcanic highlands and relatively high heat flow in older, less permeable rocks at lower elevations has been observed in the Cascade Range of northern California (*12*).

On the basis of temperature profiles from the Mt. Hood area (*9*), Newberry Volcano (*13*), and this part of the Cascades (*11*), the thickness of the nearly isothermal zone in the younger rocks generally ranges from 150 to 1000 m. In the study area only two drill holes collared in Quaternary rocks were deep enough that conductive heat flow beneath the nearly isothermal zone could be measured; the values measured were 95 mW m^{-2} (*14*) and 109 mW m^{-2} (*15*).

The temperature profiles in the Breitenbush area (Fig. 4) suggest that the high conductive heat flow measured in rocks older than 6 Ma may be a relatively shallow phenomenon. Seventeen shallow holes (<500 m deep) had high gradients that generally corresponded to heat flows >110 mW m^{-2}. However, a similar gradient in the upper part of the deepest hole (SUNEDCO 58-28) changed abruptly below a zone of thermal fluid circulation at ~800 m depth; that such a change was observed in the deepest hole suggests that the gradients in the shallow holes are also controlled by ground-water flow.

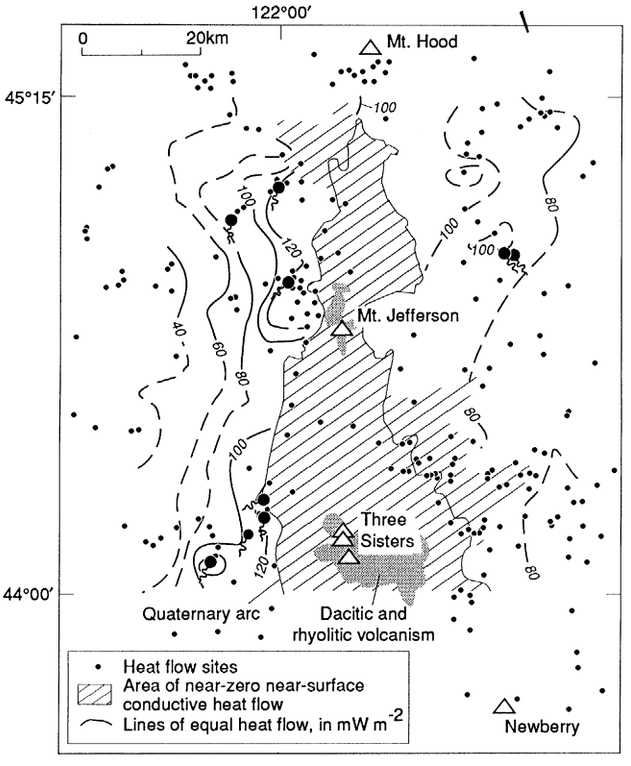

Fig. 5. Map showing lines of equal heat flow. Area of near-zero near-surface conductive heat flow in rocks younger than 6 Ma is diagonally hatched. This area is estimated conservatively; we have included in it all areas where rocks younger than 2 Ma are exposed but only included areas with rocks between 2 and 6 million years old where temperature profiles indicate that conditions are near isothermal. Areas of silicic volcanism in the Quaternary arc are shown in gray. Names of hot springs are on Fig. 1. The heat flow contours are based on 253 temperature profiles (*11*), 101 of which have also been previously published and interpreted (*7–10*).

Table 2. Components of the heat budget, in megawatts.

Deficit from area of near-zero conductive heat flow	
Quaternary arc	−399
Rocks west of Quaternary arc (2 to 6 Ma)	−18
Rocks east of Quaternary arc (2 to 6 Ma)	−40
	−457
Anomalous heat flow in rocks older than 6 Ma	
Conductive anomaly in Western Cascades	137
Advective anomaly in Western Cascades*	55
Conductive anomaly east of High Cascades	133
Advective anomaly east of High Cascades*	22
	347

*Based on discharge temperatures. The difference between the geothermometer and discharge temperatures is due to conductive heat loss (*19*) and, particularly in the Western Cascades, represents a significant fraction of the conductive anomaly.

We have used a heat budget approach (Table 2) to compare the magnitude of the heat deficit in the rocks younger than 6 Ma with that of the anomalous heat discharge in the adjacent older rocks, and to estimate the magmatic heat input required to account for the total heat flow anomaly. This analysis (Table 2) is specific to the section of the arc between 44°00′ and 45°15′N. The regional heat flow map used in our analysis is shown as Fig. 5. The conductive components of the budget are defined relative to assumed background heat flow values (*16*) and are obtained by measurement of areas on Fig. 5 with a planimeter. In general, heat flow in a given area is taken as the average of adjacent contours (for example, 70 mW m^{-2} between the 60 and 80 mW m^{-2} contours). We assigned values of 140 mW m^{-2} within the 120 mW m^{-2} contours and 60 mW m^{-2} outside the 80 mW m^{-2} contours east of the Quaternary arc.

Important assumptions in the heat budget analysis are as follows: (i) The background conductive heat flow beneath the isothermal zone in the Quaternary arc is 100 mW m^{-2}. This value is typical of areas of Quaternary volcanism (*17*) and is consistent with the two measurements in the study area. (ii) The background heat flow in Tertiary terrane is 60 mW m^{-2} (*18*). Values over 60 mW m^{-2} are the result of tectonic, magmatic, radiogenic, or hydrologic sources. (iii) The heat output of the hot springs represents the anomalous advective heat discharge from rocks older than 6 Ma. This is a minimum value because it does not include lower temperature advective discharge, which is difficult to measure.

The values for hot spring heat output used in the budget are based on discharge temperatures (T_d) rather than the geothermometer temperatures (T_g) used previously to calculate advective heat transport. The difference between T_g and T_d (Table 1) results from conductive cooling (*19*) and presumably appears as part of the conductive anomaly. In the Western Cascades, the thermal power represented by the difference between T_g and T_d (67 MW) is equal to about half of the conductive anomaly (compare the values in Fig. 1 and Table 2).

The area of near-zero near-surface conductive heat flow in this part of the Cascade Range is generally coincident with the areal extent of permeable volcanic rocks younger than 6 Ma. On the basis of our assumptions regarding background heat flow, about 460 MW of heat are swept out of these younger rocks between 44°00′ and 45°15′N by ground-water circulation. This amount is roughly balanced by 350 MW of anomalous heat discharge in the rocks older than 6 Ma (Table 2). Apparently, sufficient heat is re-

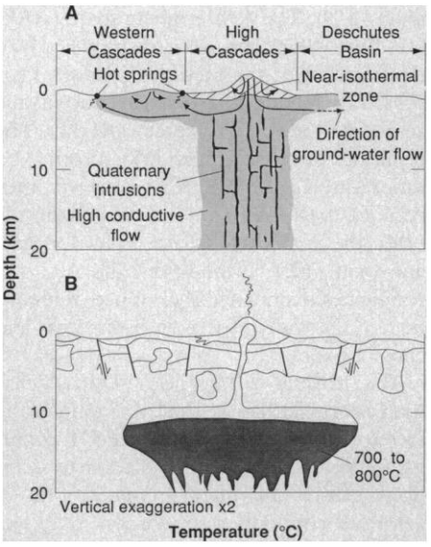

Fig. 6. (**A**) Our conceptual model of the thermal structure of the north-central Oregon Cascades, showing magmatic heat sources confined to the Quaternary arc, and (**B**) the extensive mid-crustal magmatic heat source proposed in earlier studies (for example, 7, *21, 22*).

moved advectively from the rocks younger than 6 Ma to account for the anomalous heat discharge on the flanks of the Cascade Range.

The difference between the heat deficit in the younger rocks and the anomaly in the older rocks (about 110 MW) may occur as lower temperature advective discharge, which was not determined directly. The difference between the heat deficit in the younger rocks and the heat (T_g) transported advectively by the hot spring systems (460 − 160 = 300 MW) is an estimate of the heat removed from the younger rocks by lower temperature ground-water flow or by yet-unidentified thermal fluids.

Because the anomalous heat discharge in the older (>6 Ma) rocks can be explained in terms of advection from the younger rocks, we need to invoke magmatic heat input to explain only an increment of about 40 mW m^{-2} (100 − 60 mW m^{-2}) in the background conductive heat flow beneath the Quaternary arc (an area of about 4000 km^2). This flux requires an intrusion rate of 9 to 33 km^3 per kilometer of arc length per million years (*6*). The lower intrusion rate is calculated on the basis of 900°C of magmatic cooling; the higher rate is if heat is supplied by latent heat only, with no cooling. For intermediate amounts of cooling, inferred intrusion rates scale linearly between these values. Greater rates of magmatic heat input would be expected to cause larger anomalies on the flanks of the Cascades than those observed. Because the magmatic extrusion rate has been 3 to 6 km^3 per kilometer of arc length per million years during the Quaternary (*5*), our analysis suggests that the ratio of intrusive to extrusive magma is between 1.5 and 11.

The assumption of a uniform, average heat flow value of 100 mW m^{-2} below the isothermal zone in the Quaternary arc is certainly an oversimplification. The distribution of anomalous heat discharge in the Western Cascades relative to Quaternary dacitic and rhyolitic volcanoes (Fig. 5) suggests that lateral flow of heated ground water into the Western Cascades may originate from heat sources localized near Quaternary silicic magmatic centers. The areas of silicic volcanism are presumably areas with relatively high intrusion rates, high intrusion-to-extrusion ratios, and (by inference) relatively high background heat flow (*20*).

Our conceptual model of the thermal structure of the north-central Oregon Cascades (Fig. 6A) is different from that of other workers (for example, 7, *21, 22*), who considered similar models but preferred to explain the near-surface heat flow data in terms of an extensive midcrustal magmatic heat source underlying both the Quaternary arc and adjacent older rocks (Fig. 6B). We prefer to explain the data in terms of a narrower, spatially variable deep heat-flow anomaly that expands laterally at relatively shallow depths because of ground-water flow (*23*). Confirmation of either model would require deep drilling in the areas of high heat flow in the older rocks; the actual thermal structure will undoubtedly prove more complex than either of these simple models. Our preference for the model with the narrower deep heat source (Fig. 6A) is based largely on the hot-spring data and energy-balance considerations discussed above. The intrusion rate required to support this model seems compatible with recent estimates of the Quaternary extrusion rate. Relative to the midcrustal heat source model, our model suggests that the geothermal resource base is more limited, but that the exploration target is better defined.

REFERENCES AND NOTES

1. Intrusions older than 2 Ma with volumes <1000 km^3 have almost certainly cooled to near ambient temperatures [R. L. Smith and H. R. Shaw, *U.S. Geol. Surv. Circ. 790*, 12 (1978)].
2. Our geologic data are based on a detailed compilation map of the Cascade Range prepared as part of the U.S. Geological Survey Geothermal Research Program. The Oregon sheet of this map [D. R. Sherrod and J. G. Smith, *U.S. Geol. Surv. Open-File Rep. 89-14* (1989)] is described by D. R. Sherrod, *Geotherm. Resourc. Counc. Trans.* **11**, 305 (1987). Oligocene and younger volcanic rocks are divided into 40 units on the basis of age and composition.
3. The Columbia embayment encompasses northwestern Oregon and southwestern Washington, and may be built on post-Mesozoic oceanic crust [W. Hamilton and W. B. Myers, *Rev. Geophys. Space Phys.* **4**, 509 (1966)].
4. A. J. Ellis and S. H. Wilson, *N.Z. J. Sci. Tech.* **36B**, 622 (1955).
5. D. R. Sherrod, thesis, University of California, Santa Barbara (1986).
6. For a basaltic magma with an initial temperature of 1200°C, latent heat of crystallization of 420 J g^{-1}, specific heat of 1.25 J g^{-1} °C^{-1}, density of 2.65 g cm^{-3} and cooling to ambient conditions. Values for a basaltic melt are taken from J. G. Jaeger, *Rev. Geophys.* **2**, 443 (1964); P. G. Harris, W. Q. Kennedy, C. M. Scarfe, in *Mechanism of Igneous Intrusion*, G. Newall and N. Rast; Eds. (Gallery, Liverpool, 1970), pp. 187–200.
7. D. D. Blackwell *et al.*, *J. Geophys. Res.* **87**, 8735 (1982).
8. G. L. Black, D. D. Blackwell, J. L. Steele, *Oreg. Dept. Geol. Miner. Ind. Spec. Pap.* **15**, 69 (1983).
9. J. L. Steele, D. D. Blackwell, J. M. Robison, *ibid.* **14**, 31 (1982).
10. D. D. Blackwell and S. L. Baker, *Oreg. Dept. Geol. Miner. Ind. Open-File Rep. 0-88-5*, 47 (1988).
11. S. E. Ingebritsen, R. H. Mariner, D. E. Cassidy, L. D. Shepherd, T. S. Presser, M. K. W. Pringle, L. D. White, *U.S. Geol. Surv. Open-File Rep. 88-702* (1988).
12. C. W. Mase, J. H. Sass, A. H. Lachenbruch, R. J. Munroe, *ibid. 82-150* (1982).
13. C. A. Swanberg, W. C. Walkey, J. Combs, *J. Geophys. Res.* **93**, 10163 (1988).
14. Data from a well (EWEB-2) at 44°32′41″N, 121°57′48″W that was drilled by the Eugene Water and Electric Board in 1979 and logged to a depth of 587 m. The temperature log from this hole is near-isothermal to depths of >150 m, and shows a conductive gradient of ~72°C km^{-1} below 240 m depth [W. Youngquist, *Oreg. Dept. Geol. Miner. Ind. Open-File Rep. 0-80-12* (1980)]. The heat flow estimate for this hole was published in (7) as EWEB-TM.
15. Data from a well (CTGH-1) at 44°51′02″N, 121°49′54″W that was drilled by Thermal Power Company in 1986 and logged to a depth of 1465 m. The temperature log from this hole is near-isothermal to depths of >200 m and shows a conductive gradient of ~73°C km^{-1} below 650 m depth. This hole was drilled under a cooperative agreement with the U.S. Department of Energy, and the geophysical logs from the hole were open-filed by the University of Utah Research Institute (order number CTGH-1-8). The heat flow estimate is based on an estimated thermal conductivity of 1.5 W m^{-1} K^{-1}.
16. We use the term "background heat flow" to refer to values below the depths affected by ground-water flow. The background heat flow for a given setting is determined by the competing effects of sinks (subducting slabs in this case) and sources (radioactivity and magma), and complicated by the differing thermal time constants for differing source-sink depths.
17. For example, see a study of the Japan Arc by K. Hasebe, N. Fujii, and S. Uyeda [*Tectonophysics* **10**, 335 (1970)]. We believe that this value is conservatively low, since heat flow near the younger volcanoes may locally be >>100 mW m^{-2}.
18. The global mean continental heat flow is about 60 mW m^{-2} [A. M. Jessop, M. A. Hobart, J. G. Sclater, *Geotherm. Serv. Canada Geotherm. Ser.* **5** (1976)]. The mean heat flow for Tertiary tectonic provinces is higher than 60 mW m^{-2}, with a large scatter. Thus (as beneath the Quaternary arc) the appropriate background heat flow is subject to considerable uncertainty. One could as easily use 50 or 70 mW m^{-2} (J. H. Sass, personal communication). However, our results are not particularly sensitive to the exact value assumed. For example, a background value of 50 mW m^{-2} in Tertiary terrane west of the Quaternary arc would increase the conductive anomaly from 137 (Table 2) to 178 MW.
19. Two lines of evidence suggest that the difference between the geothermometer and discharge temperatures is due to conductive cooling. First, there is a strong correlation between hot spring discharge rates and discharge temperatures (Table 1). Second, tritium data (unpublished) indicate that the thermal waters do not cool by mixing with shallow, relatively tritium-rich ground water.
20. W. Hildreth, *J. Geophys. Res.* **86**, 10153 (1981).

21. D. D. Blackwell and J. L. Steele, *Geotherm. Resourc. Counc. Trans.* 7, 233 (1983).
22. ———, *U.S. Geol. Surv. Open-File Rep. 85-521* 20, (1985).
23. Our preferred model is similar to two of the models for the Western Cascades hot springs presented by Blackwell and others (7), except that we suggest that the heat source has significant spatial variability.
24. The solubility of $CaSO_4$ provides a geothermometer which indicates maximum temperature, because few geothermal waters are saturated with gypsum or anhydrite [A. J. Ellis and W. A. J. Mahon, *Chemistry and Geothermal Systems* (Academic Press, New York, 1977)]. Anhydrite saturation temperatures for the Na-Cl and Na-Ca-Cl thermal waters that discharge in the Western Cascades correlate well with sulfate-water isotope temperatures. (R. H. Mariner, unpublished data).
25. The temperatures (T_g) listed for Kahneeta and Bagby are averages of the silica and cation geothermometers. These and other geothermometers are discussed by R. O. Fournier [in *Geothermal Systems: Principles and Case Histories*, L. Rybach and L. J. P. Muffler, Eds. (Wiley, Chichester, 1981), pp. 109–143].
26. G. R. Priest, *Oreg. Geol.* 47, 63 (1985).
27. We would like to thank numerous colleagues at the U.S. Geological Survey for helpful discussions on this topic; the advice and comments of R. J. Blakeley, T. E. C. Keith, A. H. Lachenbruch, L. J. P. Muffler, J. H. Sass, and M. L. Sorey were particularly helpful. The compilation of geologic map data relied in part on contributions from R. M. Conrey and E. M. Taylor. D. Jones drafted the figures.

20 September 1988; accepted 24 January 1989

Reduction of Intestinal Carcinogen Absorption by Carcinogen-Specific Secretory Immunity

LAWRENCE K. SILBART AND DAVID F. KEREN

A secretory immune response to the carcinogen 2-acetylaminofluorene (AAF) was elicited in rabbits by directly immunizing the small intestine with an AAF–cholera toxin conjugate. High-titer, high-affinity secretory immunoglobulin A (IgA) antibody to AAF was secreted into the intestinal lumen in response to this immunogen. Immune secretions reduced the transepithelial absorption of a ^{125}I-labeled derivative of AAF by more than half. This reduction of absorption by hapten-specific IgA suggests that oral vaccines against carcinogens and toxicants could be developed for humans.

PATHOGENIC ORGANISMS, BACTERIAL toxins, and environmental toxicants often enter the mammalian body by traversing a mucosal surface. A major mechanism to block transport at these surfaces involves the secretion of antigen-specific immunoglobulins of the IgA isotype. The protective effect conferred by the mucosal immune system is illustrated in humans by the success of a recent oral cholera vaccine containing cholera toxin B subunit and heat-killed *Vibrio cholerae* and providing immunity to the disease (*1, 2*).

We now show a mucosal immune response in rabbits to the chemical carcinogen AAF, which had a high-affinity, high-titer luminal IgA component that reduced the absorption of a radioiodinated derivative of the compound in vivo. When AAF is administered orally it is absorbed across the gastrointestinal mucosa into the blood stream and becomes a substrate for various metabolic reactions. Some metabolic pathways activate the chemical into highly reactive electrophilic intermediates capable of covalently binding to cellular macromolecules (*3, 4*). Covalent modification of nuclear DNA is believed to be an initiating event in the development of chemically induced cancer (*3, 5*).

Although a humoral immune response (IgG) can be elicited on exposure to some carcinogens (*6*), this response is substantially enhanced by covalently attaching the molecule to a foreign carrier protein (*7*). To elicit a mucosal immune response, we prepared conjugates of AAF covalently coupled to the known mucosal immunogen cholera toxin (*8, 9*). The AAF–cholera toxin (AAF-CT) mucosal immunogen was prepared by a modification of the methods published for covalently linking *N*-2-fluorenyl succinamic acid (SAF) to carrier protein (*10, 11*). The resulting conjugates had low substitution ratios (8 to 13 SAFs per CT); however, they retained their ability to bind the ganglioside GM_1 [the surface epithelial receptor for cholera toxin (*12*)]. In addition, the AAF-CT conjugates maintained their mucosal immunogenicity with respect to both AAF and cholera toxin.

The isolated rabbit ileal (Thirty-Vella) loop model (*13*) was used to monitor the secretory IgA response to AAF-CT conjugates. We collected daily intestinal secretions before and after immunizations. A vigorous antibody response to AAF was observed in the intestinal secretions collected from all immunized rabbits, with material obtained from three of four rabbits binding more than 10% of an iodinated radiotracer [^{125}I-labeled *N*-2-(4-hydroxyphenyl)acetamidofluorene or ^{125}I-pHP-AAF (*10*)] offered at titers of 10^3 (nonspecific binding to nonimmune secretions was less than 2%). The epitope and isotype specificity of the mucosal immune response was determined by competitive enzyme-linked immunosorbent assay [ELISA (*10*)]. In these studies, incubation of 1:20 dilutions of ileal loop secretions in the presence of AAF inhibited binding to the AAF–carrier protein conjugates in a concentration-dependent manner (Fig. 1), indicating antibody recognition of the AAF epitope on the AAF-CT conju-

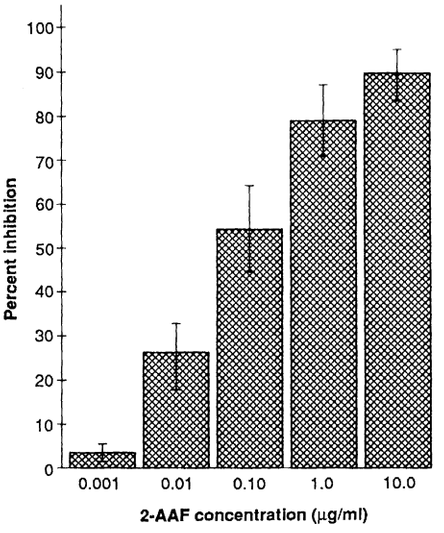

Fig. 1. The IgA anti-AAF isotype and epitope specificity were determined in rabbit intestinal secretions by competitive ELISA studies as described (*10*) with goat antibody to rabbit IgA (affinity purified) conjugated to alkaline phosphatase [GARA (*14*)]. The AAF was preincubated with 1:20 dilutions of immune secretions for 1 hour at room temperature. A 100-μl sample was applied in duplicate to microtiter wells previously coated with either AAF–bovine serum albumin (BSA) conjugates, BSA alone, or uncoated wells. After a 4-hour incubation at room temperature, the plates were washed and treated with GARA overnight. After washing, the *p*-nitrophenyl phosphate (1 mg/ml) was added, and the absorbance was measured (405 nm) after 100 min. The percent inhibition was calculated on the basis of 0% for wells containing no AAF. Values represent the mean inhibition ± SE ($n = 4$) after subtraction of absorbance in the corresponding BSA wells (nonspecific binding). AAF had no effect on unrelated antigen-antibody interactions over the range of concentrations tested (*15*). Since the AAF stock solution was prepared in dimethylformamide (DMF), DMF control (5% and 0.5%) incubations with the uninhibited immune secretions were included on each plate and used in the appropriate calculations. The secretory immune response to AAF was elicited by the following regimen: four rabbits received 100 μg of the AAF-CT conjugate in 1 ml of phosphate-buffered saline (PBS) directly into a chronically isolated ileal loop approximately 3 hours after the ileal loop surgery. Identical booster doses were given on days 7, 14, and 21 after the surgery and priming dose. The immune response of each rabbit was initially measured by the binding of an ^{125}I derivative of AAF in a radioimmunoassay method as described (*10*).

University of Michigan, Pathology Department, Ann Arbor, MI 48109.